The Phase Diagrams of the Systems Na_3AlF_6-$Fe_{0.947}O$ and Na_3AlF_6-FeF_2 and Related Activities of FeF_2 from Emf Measurements

Helge Grini Johansen,[a] Åsmund Sterten[b,*] and Jomar Thonstad[b]

[a]Hydro Aluminium Offshore a.s., N-4262 Avaldsnes and [b] Laboratories of Industrial Electrochemistry, The Norwegian Institute of Technology, N-7034 Trondheim-NTH, Norway

Johansen, H. G., Sterten, Å. and Thonstad, J., 1989. The Phase Diagrams of the Systems Na_3AlF_6-$Fe_{0.947}O$ and Na_3AlF_6-FeF_2 and Related Activities of FeF_2 from Emf Measurements. – Acta Chem. Scand. 43: 417–420.

The systems Na_3AlF_6-FeF_2 and Na_3AlF_6-$Fe_{0.947}O$ were studied by thermal, chemical and X-ray analysis. Both Na_3AlF_6-FeF_2 and Na_3AlF_6-$Fe_{0.947}O$ constitute simple eutectic systems. The eutectic points are located at 73 ± 2 mol % FeF_2 and 1016 ± 3 K, and at 14.2 ± 0.5 mol % $Fe_{0.947}O$ and 1256 ± 2 K in the respective systems. The electrodes in the cell

Pt |Fe|FeF_2(l), Na_3AlF_6(l)|H_2(g), HF(g)|Pt

were found to behave reversibly. The emf data were used to estimate activities of FeF_2 in liquid Na_3AlF_6. A negative deviation from ideality was observed, indicating the presence of complex-bound iron ions in the melt.

This paper encompasses phase diagram studies of the systems Na_3AlF_6-FeF_2 and Na_3AlF_6-Fe_xO, together with emf measurements on the cell

$$Pt|Fe|FeF_2,\ Na_3AlF_6|HF,\ H_2|Pt \qquad (1)$$

This work was undertaken in connection with a study of the behaviour of iron impurities in the aluminium production process.[1] The iron which contaminates the produced metal enters the process through the raw materials and by corrosion of steel parts and tools. In the electrolyte it can be present as tri- or divalent iron. The present study was focused on the properties of divalent iron in the system. Solubility and activity data were needed in order to assess the extent and the nature of dissolved Fe(II) species in the melt. To our knowledge phase diagram data for the Na_3AlF_6-FeF_2 and the Na_3AlF_6-Fe_xO systems have not been reported in the literature. One of the main purposes of this investigation was to test the H_2, HF|Pt electrode for use in cryolitic melts, and to derive activity data. Hitch and Baes[2] have successfully applied such an electrode in molten mixtures of BeF_2 and LiF. Ema *et al.*[3] used the HF|H_2|Pt electrode as a reference electrode in a molten LiF-KF mixture.

Experimental

Chemicals. Hand-picked natural Greenland cryolite (Na_3AlF_6) with a melting point of 1284 K was employed. The iron impurities in this mineral were analysed and found to constitute 0.003 % by weight. An iron crucible with a purity of 99.94 % Fe was used in most of the phase diagram studies, while a graphite crucible was employed in the emf measurements. Fe_xO was prepared by fusing a mixture of Na_3AlF_6 and Fe_2O_3 (min. 99 %) in the iron crucible, according to the equation:

$$Fe_2O_3(diss) + (3x-2)\ Fe(s) = 3\ Fe_xO(diss) \qquad (2)$$

The mixture was stirred in order to accelerate the reaction. The oxide composition at equilibrium with iron was taken to be $Fe_{0.947}O$ in the temperature range 1200 to 1300 K.[4]

FeF_2 in solution was prepared in a similar way allowing FeF_3 to equilibrate with the iron crucible containing molten cryolite:

$$2\ FeF_3(diss) + Fe(s) = 3\ FeF_2(diss) \qquad (3)$$

Thus, both FeF_2 and $Fe_{0.947}O$ were prepared *in situ* during the experiments. However, a commercially available FeF_2 (92–96 %) powder which had been vacuum-treated at 700 K was employed in the emf measurements. The iron plate electrode used in the emf measurements had a purity of 99.99 %. Anhydrous hydrogen (99.995 %) and HF (99 %) were used without further purification.

Apparatus and procedures. The thermal analysis was performed in a conventional vertical tube furnace. Supercooling of the melt was minimized by vigorous stirring, use of a slow cooling rate in the range 0.5–1.0 K min^{-1}, and frequent addition of small cryolite seed crystals to the molten mixture. The temperature of the melt in all measurements was determined by means of a calibrated Pt-Pt, 10 % Rh thermocouple. A thermal analysis experiment was started by determining the melting point of pure cryolite, whereafter the liquidus temperature was determined after each

* To whom correspondence should be addressed.

subsequent addition of oxide or fluoride. The liquidus temperature for a given composition was usually determined twice, and always from cooling curves, to see whether the equilibrium reactions (2) or (3) were complete.

The liquidus composition at a given temperature was in some cases determined by chemical analysis of samples taken from the melt. The samples were fused in a soda-borax mixture in a platinum crucible. The solidified product was dissolved in dilute H_2SO_4, whereafter pH was adjusted to about 3.5 by addition of sodium acetate. The amount of iron(II) complexes was then determined colorimetrically after addition of *o*-phenanthroline. Subsequently, the content of Fe^{3+} was reduced to Fe^{2+} with hydroxylamine hydrochloride, whereafter the total amount of iron (as Fe^{2+}) was determined colorimetrically. In this way the content of both Fe^{2+} and Fe^{3+} in the original samples could be determined.

The cell used for the emf measurements was separated into two compartments by an open-ended graphite tube placed about 0.5 cm above the bottom of the container. The H_2, HF|Pt electrode consisted of a platinum tube perforated at the end and dipping into the melt inside the graphite tube, which also served to collect the gas mixture (H_2, HF) leaving this compartment. The other electrode, which consisted of an iron platelet, was immersed in the melt outside the graphite tube. This experimental arrangement provided good contact between the electrodes and satisfactory mixing of the electrolytes in the two compartments.

The H_2, HF gas mixture was prepared by bubbling H_2 through liquid HF contained in a thermostatted copper vessel outside the furnace. Due to the corrosiveness of HF, the cold part of the gas support equipment was made exclusively of copper, teflon and inconel, and the hot parts of platinum and graphite. The HF vapour pressure in the exit gas from the gas electrode compartment was determined by alkalimetric titration. The iron content of the melt after each addition of FeF_2 was also determined analytically as described above.

Results and discussion

Phase diagram studies. Fig. 1 shows the cryolite-rich part of the Na_3AlF_6-Fe_xO phase diagram in the range 1250 to 1300 K. X-Ray analysis of quenched samples from a 30 mol % Fe_xO + 70 mol % Na_3AlF_6 mixture kept at 1300 K and vigorously stirred for about 4 hours showed that the phases Na_3AlF_6, Fe_xO and possibly Fe_3O_4 were present at room temperature. Fe_3O_4 is most probably formed by a disproportionation reaction of Fe_xO during cooling, since this compound is thermodynamically unstable[5] below about 843 K. The results indicate that Na_3AlF_6-Fe_xO is a binary system above that temperature. The cryolite liquidus line was determined by thermal analysis, while the iron oxide liquidus line was found by analysis of the iron content of melts saturated with Fe_xO as explained above. The two liquidus curves, established by different methods, and the

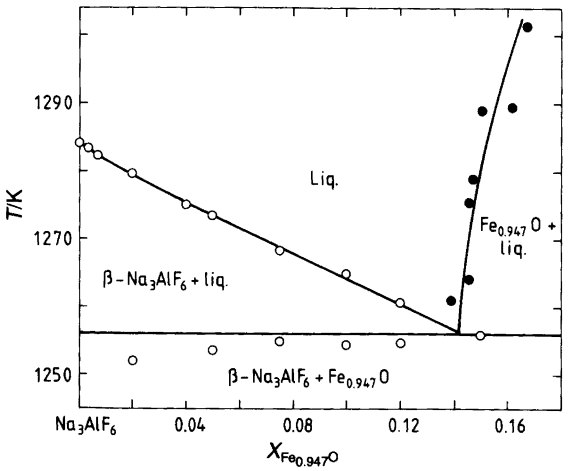

Fig. 1. The cryolite-rich part of the phase diagram for Na_3AlF_6-$Fe_{0.947}O$. ○: from thermal analysis. ●: from chemical analysis.

solidus line intersect at the eutectic composition 14.2 ± 0.5 mol % $Fe_{0.947}O$ at 1256 ± 2 K, as shown in Fig. 1. This relatively high solubility of Fe_xO in cryolite is noteworthy, since the equilibrium

$$3\ \text{"FeO"} + 2\ Na_3AlF_6 = Al_2O_3 + 3\ NaF \cdot FeF_2 + 3\ NaF \quad (4)$$

is displaced to the left when the compounds are in the solid state. $NaF \cdot FeF_2$ is a stable compound in the Na_3AlF_6-NaF-FeF_2 system.[6]

The results depicted in Fig. 2 show that Na_3AlF_6-FeF_2 constitutes a simple eutectic system. X-Ray diffraction studies of quenched samples from molten mixtures showed peaks only for Na_3AlF_6 and FeF_2. The cryolite liquidus line down to 45 % Na_3AlF_6 was established by thermal analysis. The extension down to the eutectic composition fits nicely to the points determined by chemical analysis of iron. The eutectic point (1016 ± 3 K and 73 ± 2 mol % FeF_2) appears from the data given in Fig. 2 to be well defined. The

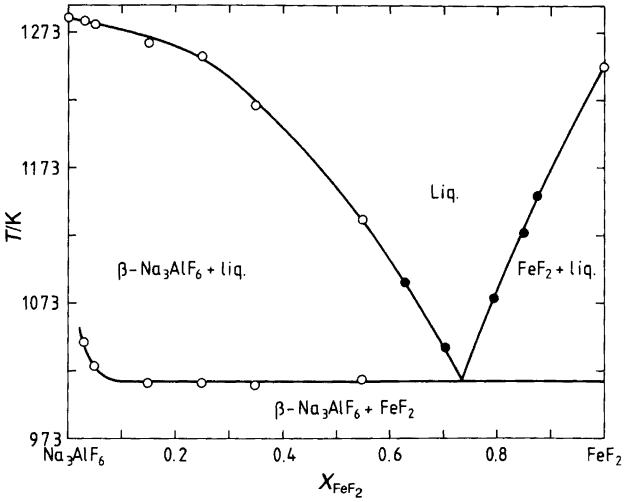

Fig. 2. The system Na_3AlF_6-FeF_2. ○: from thermal analysis. ●: from chemical analysis.

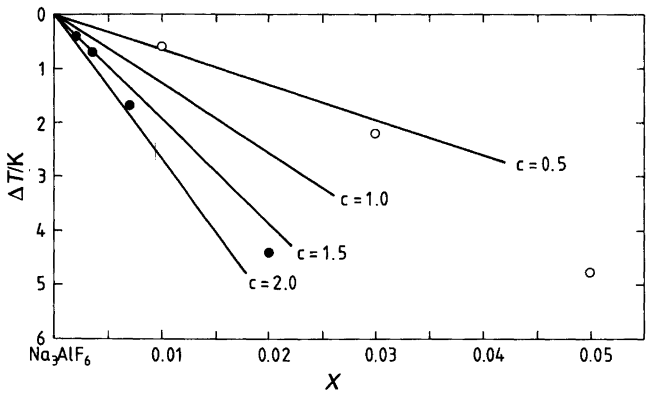

Fig. 3. Freezing point depression data for the systems Na_3AlF_6-FeF_2 and Na_3AlF_6-$Fe_{0.947}O$ compared to calculated liquidus lines for the formation of *c* units of foreign species by the addition of one unit of the iron compounds. ○: points for the system Na_3AlF_6-FeF_2. ●: points for the system Na_3AlF_6-$Fe_{0.947}O$.

upward bend of the solidus line at low contents of FeF_2 may indicate a minor solid solubility of FeF_2 in Na_3AlF_6. The melting point of FeF_2 was found to be T_m = 1248 ± 3 K, roughly in agreement with the melting point shown in a phase diagram reported by Samouel.[7] Some values for the melting point reported elsewhere[4,8,9] are obviously in error.

An extensive analysis of Na_3AlF_6-M_xO_y phase diagrams has revealed that the cryolite liquidus line can be reproduced rather accurately by calculating the freezing point depression using known activity data and the heat of melting of cryolite, i.e. ΔH_m^0 = 106.745 kJ mol^{-1}.[10,11] Fig. 3 shows freezing point depressions calculated for a number of different foreign species[10] assuming no solid solubility. The experimental results indicate that the numbers of new entities formed at infinite dilution are approximately 0.5 and 1.5 for FeF_2 and Fe_xO, respectively. These numbers are somewhat unexpected since the solid solubilities are rather small. A dimerization of iron ions in cryolitic melts may explain the numerical values, since the oxygen atoms most probably will form one new species. However, more information is needed in order to draw more definite conclusions about the structure of these melts.

Emf measurements. The H_2/HF vapour pressure ratio was found to vary somewhat with time during the emf measurements. The gas composition was therefore determined for each emf measurement as indicated in Table 1. The other data in the table are discussed below.

Two identical iron electrodes located in the same compartment were used in one single run. One of these electrodes was short-circuited with the H_2/HF electrode for about half a minute. The open circuit potential subsequently regained its original value within a few minutes. The potential difference between the iron electrodes was stabilized at ± 1 mV. These observations indicate that the cell reaction

$$Fe(s) + 2\ HF(g) = FeF_2(diss) + H_2(g) \qquad (5)$$

is reversible and gives rise to reproducible emf values.

Table 1. Emf data for cell (1) from three series of experiments, see text. *X* is the mole fraction of FeF_2. p_1 and p_2 are the partial pressures of HF and H_2, respectively, while *a* and γ are the activity and the activity coefficient, respectively, of FeF_2. Temperature: 1293 K.

Series	*X*	*E*/mV	p_1/atm	p_2/atm	*a*	γ
1	0.0127	244	0.58	0.42	0.0022	0.174
1	0.0197	233	0.62	0.38	0.0034	0.173
1	0.0364	197	0.62	0.38	0.0065	0.179
2	0.0069	316	0.70	0.30	0.0012	0.180
2	0.0109	288	0.68	0.32	0.0018	0.167
2	0.0164	260	0.68	0.32	0.0030	0.183
2	0.0217	253	0.69	0.31	0.0036	0.167
2	0.0327	222	0.68	0.32	0.0060	0.182
2	0.0415	209	0.68	0.32	0.0075	0.181
2	0.0601	183	0.67	0.33	0.0113	0.188
2	0.0740	170	0.67	0.33	0.0142	0.192
3	0.0199	239	0.63	0.37	0.0033	0.164
3	0.0396	200	0.63	0.37	0.0066	0.165
3	0.0561	167	0.60	0.40	0.0105	0.187
3	0.0753	145	0.60	0.40	0.0155	0.206
3	0.0833	133	0.62	0.38	0.0206	0.247
3	0.1002	122	0.62	0.38	0.0251	0.250

Three series of runs were performed. Emf values and corresponding melt compositions are presented in Table 1. In order to calculate activity data from the emf equation

$$E = E^0 - (RT/nF)\ln(a_{FeF_2} \cdot p_{H_2}/p^2_{HF}) \quad (6)$$

the standard emf of the cell reaction, E^0, must be known.

The reaction

$$FeF_2(diss) + HF(g) = FeF_3(diss) + 1/2\ H_2(g) \quad (7)$$

is expected to proceed slightly to the right in pure liquid FeF_2. This means that an accurate determination of E^0 by use of cell (1) using pure FeF_2 is hard to achieve. The standard Gibbs energy of formation of liquid FeF_2 is estimated in the Janaf Tables[4] to be -525 ± 42 kJ mol^{-1} at 1293 K. Using recent data we have tried to evaluate a more accurate value. Chattopadhyay *et al.*[12] and Azad *et al.*[13] have derived the following two equations for the Gibbs energy of formation of solid FeF_2

$$\Delta G^0_f/\text{kJ mol}^{-1} = -701.745 + 0.1238\ T \pm 2.5 \quad (8)$$

$$\Delta G^0_f/\text{kJ mol}^{-1} = -702.000 + 0.12520\ T \pm 0.70 \quad (9)$$

The entropy of melting for FeF_2, $\Delta S^0_m = 38$ J mol^{-1} K^{-1}, was taken from the Janaf Tables.[4] The heat of melting, $\Delta H^0_m = 47.424$ kJ mol^{-1}, was derived using $T_m = 1248$ K from the present work. Combining these values with eqns. (8) and (9) gives $\Delta G^0_f = -542.55$ kJ mol^{-1} as an average value for liquid FeF_2 at 1293 K. The standard emf of the cell reaction (5) is then computed as $E^0 = -0.084$ V at 1293 K using Gibbs energy data for HF(g) from the Janaf Tables.[4] The activity data derived from eqn. (6) on this basis are collected in Table 1. The uncertainty in the activity data is difficult to estimate, but it is believed to be within 50 % of the given values. Further work is needed in order to obtain more reliable thermodynamic data for liquid FeF_2.

In spite of these uncertainties it can be concluded that the negative deviation from ideal Raoult's law behaviour indicates interaction of iron ions in the melt. This conclusion is in agreement with the phase diagram data discussed above.

Acknowledgement. Financial support from the Royal Norwegian Council for Scientific and Industrial Research and from *Mosjćen Aluminiumverk* is gratefully acknowledged.

References

1. Johansen, G. H., Thonstad, J. and Sterten, Å. *Light Met.* (1977) 253.
2. Hitch, B. F. and Baes, C. F. *Inorg. Chem. 8* (1969) 201.
3. Ema, K., Ito, Y., Takenaka, T. and Oishi, J. *Electrochim. Acta 32* (1987) 1537.
4. Stull, R. D. and Prophet, H. *Janaf Thermochemical Tables,* 2nd ed., NSRDS-NBS 37, Washington, D.C. 1971.
5. Adams, D. M. *Inorganic Solids,* Wiley, New York 1981.
6. Johansen, G. H. *Dissertation,* Laboratories of Industrial Electrochemistry, University of Trondheim, Trondheim, Norway 1975.
7. Samouel, M. *Rev. Chim. Miner. 8* (1971) 545.
8. Tsiklauri, Ts. G., Ippolitov, E. G., Zhigarnovskii, B. M. and Petrov, S. V. *Soobschch. Akad. Nauk Gruz. SSR 69* (1973) 593; cited in Roth, R. S., Negas, T. and Cook, L. P., Eds., *Phase Diagrams for Ceramicists,* The American Ceramic Society, Columbus, Ohio 1983, Vol. V, fig. 5783.
9. Biltz, W. and Rahlfs, E. *Z. Anorg. Allgem. Chem. 166* (1927) 363.
10. Sterten, Å. and Mæland, I. *Acta Chem. Scand., Ser. A 39* (1985) 241.
11. Sterten, Å. and Skar, O. *Aluminium 64* (1988) 1051.
12. Chattopadhyay, G., Karkhanavala, M. D. and Chandrasekharaiah, M. S. *J. Electrochem. Soc. 122* (1975) 325.
13. Azad, A. M. and Sreedharan, O. M. *J. Appl. Electrochem. 17* (1987) 949.

Received September 30, 1988.